Available online at www.eccomasproceedia.org
Eccomas Proceedia COMPDYN (2023) 2009-2016

ECCOMAS
Proceedia

COMPDYN 2023
9th ECCOMAS Thematic Conference on
Computational Methods in Structural Dynamics and Earthquake Engineering
M. Papadrakakis, M. Fragiadakis (eds.)
Athens, Greece, 12-14 June 2023

ON THE RESPONSE OF SDOF RATE-INDEPENDENT HYSTERETIC MECHANICAL SYSTEMS SUBJECTED TO SHOCK EXCITATION

D.F. Ledezma-Ramirez[1], **P.E. Tapia-Gonzalez**[1] **and N. Vaiana**[2]

[1] Universidad Autónoma de Nuevo León, Facultad de Ingeniería Mecánica y Eléctrica,
Centro de Investigación e Innovación en Ingeniería Aeronáutica,
San Nicolás de los Garza, Nuevo León, México

[2] University of Naples Federico II, Department of Structures for Engineering and Architecture, Napoli, Italy

e-mail: diego.ledezmard@uanl.edu.mx

Abstract

The hysteretic behavior of mechanical systems is intrinsically nonlinear since their output not only depends on the current value of the input but also on its history. Specifically, such systems exhibit a rate-independent hysteretic behavior when the generalized force does not depend on the rate of variation of the applied generalized displacement.
According to the type of shape, characterizing their typical generalized force-displacement hysteresis loops, it is possible to distinguish between mechanical systems with symmetric and asymmetric hysteretic behavior. In the former case, a typical hysteresis loop may be described by its loading curve (upper bound) having the same shape of the unloading curve (lower bound). On the contrary, in the latter case, a typical hysteresis loop may be described by generic loading and unloading curves and/or upper and lower bounds having different shapes.
In this work, the response of several Single-Degree-Of-Freedom (SDOF) rate-independent hysteretic mechanical systems is investigated, characterized by different types of symmetric or asymmetric hysteresis loop shapes, when they are subjected to a shock excitation considering a symmetrical half-cycle sine pulse of different durations. The obtained results will be helpful to designers and researchers working in the field of aerospace, civil, and mechanical engineering.

Keywords: Shock response, hysteresis, shock isolation, nonlinear isolator.

ISSN:2623-3347 © 2023 The Authors. Published by Eccomas Proceedia.
Peer-review under responsibility of the organizing committee of COMPDYN 2023.
doi: 10.7712/120123.10538.20958

1 INTRODUCTION

Vibrations produced from mechanical shock and impact are a usual phenomenon in military, naval, aerospace and transport applications and can result in negative effects such as fatigue, noise and wear. In order to reduce these effects resilient mounts are used. These mounts store the impact energy when deformed which is subsequently dissipated by damping [1]. In the same trend, earthquake ground motion provides a shock-type excitation under near-field conditions thus significantly increasing displacement demand on base isolation systems [2, 3, 4]. In case of frame buildings, a valuable solution is provided by supplemental dampers on mounting braces [5, 6]. Nevertheless, isolation effectiveness usually comes with the cost of a large deformation of the support, thus requiring considerable space to allow for large relative motion. The loading and unloading of such isolators can result in hysteresis loops of the force-deformation curves, which can be symmetric or asymmetric depending on a particular configuration, load type and rate. Predicting the shock response of such isolators is important since several of the commercially available shock mounts exhibit such hysteretic behaviour when subjected to large deformations during cyclic loading. For instance, wire rope isolators (WRIs), also known as cable isolators are particularly prone to this. These isolators are capable of high energy storage and dissipation in a compact package. Their stiffness characteristics are nonlinear due to the spring configuration and energy dissipation is due to the dry friction created between the wire strands as the cable twists during loading and unloading of the isolator. These effects result in hysteresis behaviour under cyclic loading [7]. Despite of their use as shock isolators, most of the isolation designs based on wire ropes are empirical or based in classic isolation theory, which does not reflect the nonlinear properties typically observed in these isolators. Thus, in this work, a rate independent model for predicting the symmetric and asymmetric hysteresis is applied to a single degree of freedom system under a half sine shock pulse, in order to theoretically study the shock response. It is expected that the results obtained can lead to a better prediction and design of shock isolators with hysteretic behaviour.

2 ADOPTED HYSTERETIC MODEL

In this Section, we first summarize the formulation of the adopted uniaxial hysteretic model belonging to a more general class introduced by Vaiana et al. [8, 9, 10]; subsequently, we illustrate the different types of hysteresis loop shapes that can be reproduced by means of the model which is based on a set of only six parameters: k_a, k_b, α, β_1, β_2, and γ.

2.1 Model Formulation

In the adopted hysteretic model, u (f) represents the generalized displacement (force), whereas $\dot{u}$ is the generalized velocity.

The generalized force, during the generic loading case ($\dot{u} > 0$), is evaluated as:

$$f\left(u,u_j^+\right) = \begin{cases} c^+\left(u,u_j^+\right) & u \in \left[u_j^+ - 2u_0,\ u_j^+\right] \\ c_u\left(u\right) & u \in \left[u_j^+,\ \infty\right) \end{cases}, \tag{1}$$

whereas, during the generic unloading case ($\dot{u} < 0$), it is computed as:

$$f\left(u,u_j^-\right) = \begin{cases} c^-\left(u,u_j^-\right) & u \in \left[u_j^-,\ u_j^- + 2u_0\right] \\ c_l\left(u\right) & u \in \left(-\infty,\ u_j^-\right] \end{cases}. \tag{2}$$

In the previous two equations, c^+ and c^- represent, respectively, the generic loading and unloading curves:

$$c^+(u,u_j^+) = -(\beta_1+\beta_2)u + e^{\beta_1 u} - e^{-\beta_2 u} + e^{\gamma u}\left\{k_b u - \frac{k_a-k_b}{\alpha}\left[e^{-\alpha\left(+u-u_j^+ +2u_0\right)} - e^{-2\alpha u_0}\right] + f_0\right\}, \quad (3)$$

$$c^-(u,u_j^-) = -(\beta_1+\beta_2)u + e^{\beta_1 u} - e^{-\beta_2 u} + e^{\gamma u}\left\{k_b u + \frac{k_a-k_b}{\alpha}\left[e^{-\alpha\left(-u+u_j^- +2u_0\right)} - e^{-2\alpha u_0}\right] - f_0\right\}, \quad (4)$$

whereas c_u and c_l are, respectively, the upper and lower limiting curves:

$$c_u(u) = -(\beta_1+\beta_2)u + e^{\beta_1 u} - e^{-\beta_2 u} + e^{\gamma u}\left(k_b u + f_0\right), \quad (5)$$

$$c_l(u) = -(\beta_1+\beta_2)u + e^{\beta_1 u} - e^{-\beta_2 u} + e^{\gamma u}\left(k_b u - f_0\right). \quad (6)$$

The internal variable u_j^+ (u_j^-), that represents the displacement value where the generic loading (unloading) curve intersects the upper (lower) limiting curve, is given by:

$$u_j^+ = u_P + 2u_0 + \frac{1}{\alpha}\ln\left\{\frac{\alpha}{k_a-k_b}\left[e^{-\gamma u_P}\left(-(\beta_1+\beta_2)u_P + e^{\beta_1 u_P} - e^{-\beta_2 u_P}\right) + k_b u_P + \frac{k_a-k_b}{\alpha}e^{-2\alpha u_0} + f_0 - e^{-\gamma u_P} f_P\right]\right\}, \quad (7)$$

$$u_j^- = u_P - 2u_0 - \frac{1}{\alpha}\ln\left\{\frac{-\alpha}{k_a-k_b}\left[e^{-\gamma u_P}\left(-(\beta_1+\beta_2)u_P + e^{\beta_1 u_P} - e^{-\beta_2 u_P}\right) + k_b u_P - \frac{k_a-k_b}{\alpha}e^{-2\alpha u_0} - f_0 - e^{-\gamma u_P} f_P\right]\right\}, \quad (8)$$

in which u_P and f_P are the coordinates of a generic point P belonging to c^+ or c^-.

Finally, the internal parameters f_0 and u_0 are evaluated as:

$$f_0 = \frac{k_a-k_b}{2\alpha}\left(1-e^{-2\alpha u_0}\right), \quad (9)$$

$$u_0 = -\frac{1}{2\alpha}\ln\left(\frac{\delta_k}{k_a-k_b}\right), \quad (10)$$

where δ_k is a numerical parameter set equal to 10^{-20}, whereas k_a, k_b, α, β_1, β_2, and γ represent the six model parameters to be calibrated from experimental or numerical data, with $k_a > k_b$, $k_a > 0$, $\alpha > 0$, $\beta_1 \geq 0$, $\beta_2 \geq 0$, and γ real.

2.2 Hysteresis loop shapes

Figure 1 shows the six different types of generalized force-displacement hysteresis loop shapes that can be reproduced by means of the proposed model. Note that, in this paper, the parameter γ is set equal to 0 for brevity. More details can be found in [9].

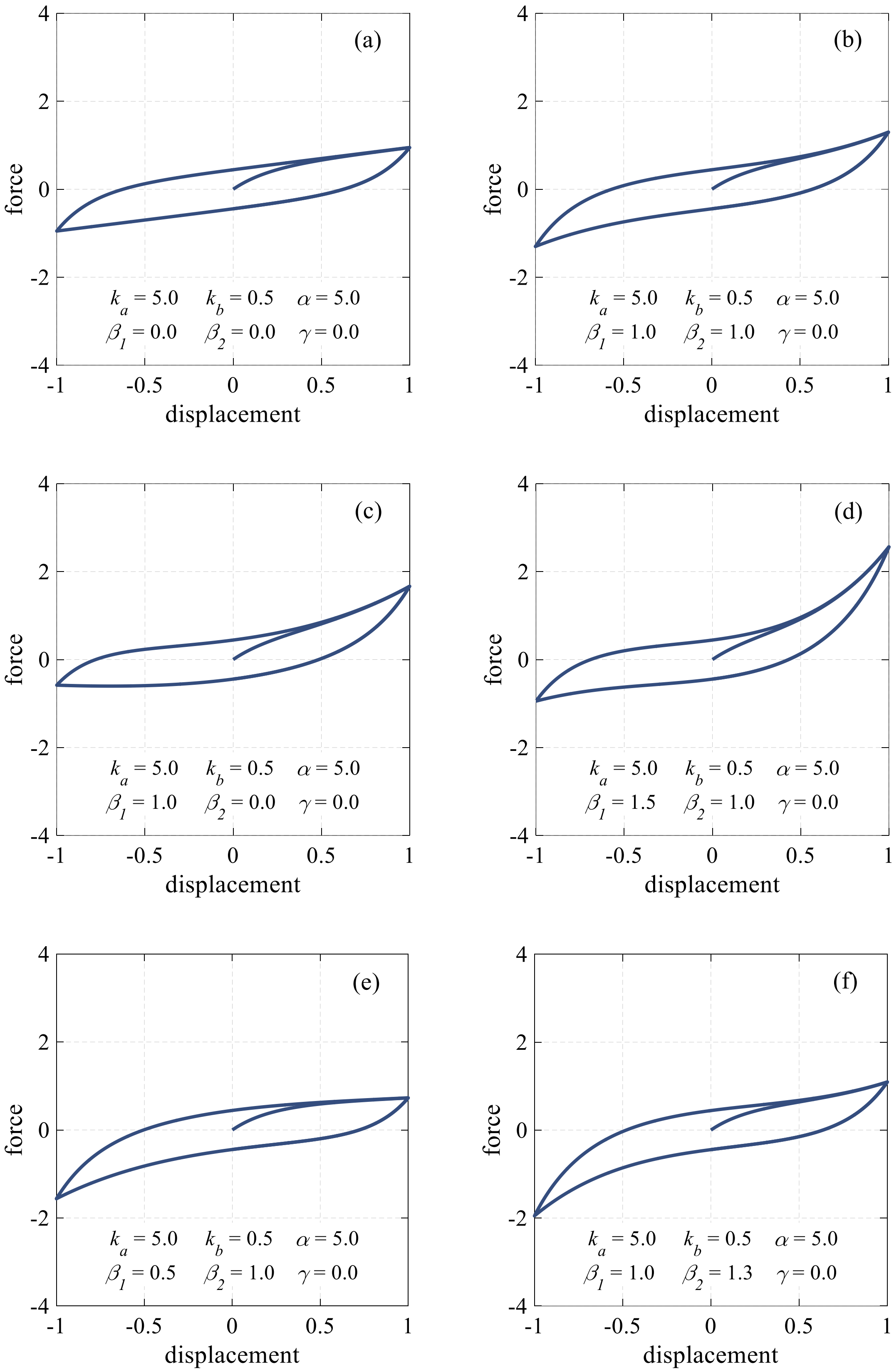

Figure 1: Types of hysteresis loop shapes that can be simulated by using the adopted hysteretic model.

3 SHOCK RESPONSE

3.1 Description of shock input and response spectra

The response of shock vibration is characterized by performance indices such as absolute and relative displacement of the isolated mass, which are indicators of the space available or needed, and the maximum acceleration related to the transmitted forces. A period ratio is introduced as the duration of the impact compared to the natural period of the isolation system, commonly modelled as a mass spring damper system (MKC). The shock response is classified into three different categories according to the period ratio. When the duration of the impact is short, i.e. less than half the natural period the response is impulsive and its magnitude is smaller compared to the input. In addition, maximum response occurs once the impact is over. When the duration of the impact is approximately equal to the natural period, the response is amplified. For pulses greater than twice the natural period, the excitation is applied slowly, and it is considered quasistatic. These responses can be summarized in a plot called "Shock Response Spectra" or SRS [11]. Figure 2 shows an example of SRS for a system of one degree of freedom with low damping, subject to a half sine acceleration pulse applied to the base. The vertical axis represents the maximum response of the system $\ddot{x}_m$ normalized to the maximum amplitude of the input $\ddot{y}_p$, and the horizontal axis represents the relative ratio of the pulse duration. The maximax, i.e. maximum response at any time either during the application of the pulse or once it has finished, and the relative response between base and payload mass are depicted by the black and red lines respectively.

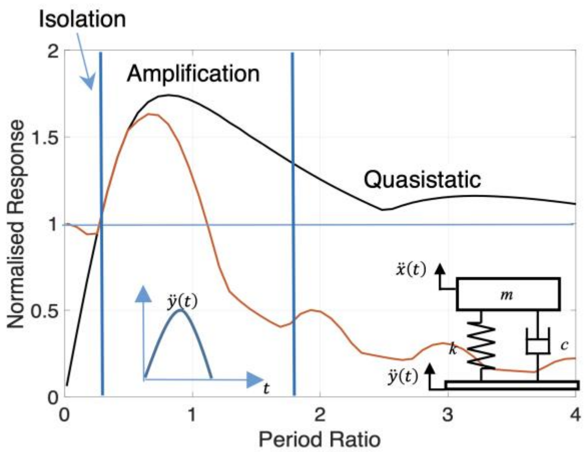

Figure 2. Shock Response Spectrum (SRS) for a MKC model under a half sine acceleration pulse. The black line represents the maximax acceleration response whilst the red line represents relative motion.

3.2 Shock response of the hysteresis model

In this section, the shock response of the asymmetrical exponential model of hysteresis is presented. A single degree of freedom model where the restoring force is given by the generalized force of the hysteresis model is considered, whilst the model is under a base acceleration in the form of a half sine pulse excitation of different durations. The equation of motion of the model is given by Equation 11 where $f(u)$ represents the generalized hysteretic force, $\ddot{y}$ is the input amplitude of the half sine pulse and τ its duration. Then, the maximum response is evaluated and presented in the form of a response spectra in Figure 3. The response of the system is numerically evaluated in MATLAB using an ODE solver. The hysteresis model parameters are those presented in the loops of Figure 1.

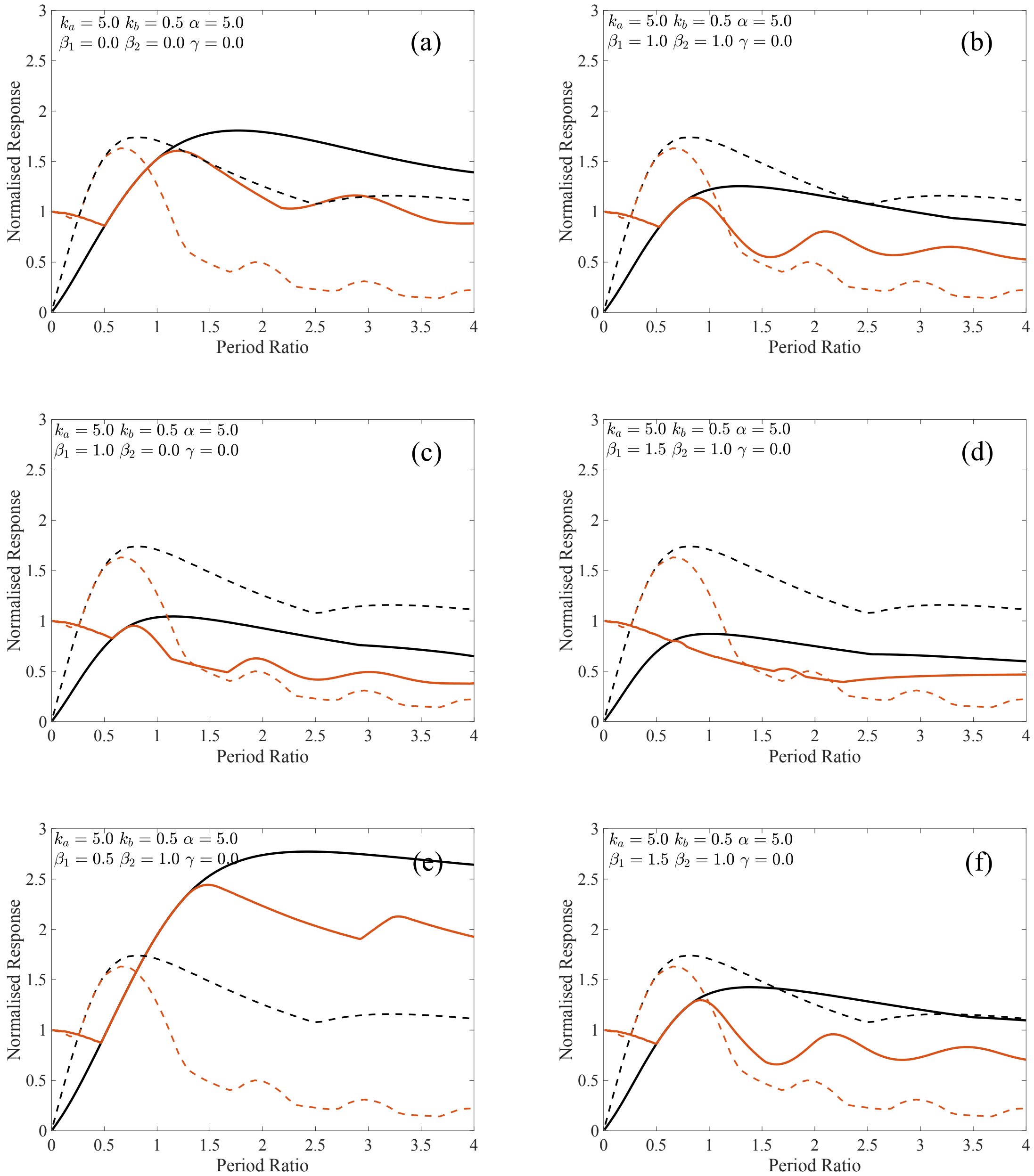

Figure 3: Shock response spectra for the loops indicated in Figure 1.
(— Maximax response hysteresis model, - - maximax response MKC model, — relative response hysteresis model, - - relative response MKC model)

$$m\ddot{x} + f(u) = \ddot{y}\sin\left(\frac{\pi t}{\tau}\right) \tag{11}$$

In Figure 3, maximax and relative responses for the hysteresis model are depicted by the continuous black and red lines respectively, whilst the broken lines represent the response of a lightly damped MKC model for reference. In all cases, the isolation zone of the SRS is shifted towards the region of longer pulses, allowing for improved isolation in a wider range. Relative motion in this extended isolation area is still similar to that of the MKC model, since isolation relies on the energy absorption by deformation of the elastic element. It is important to note that isolation is vastly improved for longer pulses in most of the presented cases, which is an advantage over the MKC model. It is possible that the improved isolation relies on the energy dissipation phenomena due to the hysteresis effect, since the effect is similar to the response spectra of heavily damped MKC models [11]. Only one case presents a larger response compared to the MKC model, perhaps due to the softening effect observed in the hysteresis loop, which is adequate for short duration pulses, but allows for larger responses in longer pulses.

4 CONCLUSSIONS

This paper presented an overview of an asymmetric exponential model to reproduce hysteresis behaviour. Such model is particularly well suited to represent a variety of hysteresis loop shapes and several examples were presented based on the selection of the model parameters. Then, the shock response of the presented loop examples was numerically calculated considering a single degree of freedom model with a restoring force provided by the hysteresis model. Improved shock isolation was found for a wider range of shock durations compared to the classic spring mass damper model. This model can provide a better prediction of the response in commercial shock isolators such as wire rope springs that present a variety of hysteresis loops depending on the type of load applied. Further validation based on the properties of actual isolators and experimental testing is suggested for future work that can lead to better approximation of the response.

REFERENCES

[1] D.F. Ledezma-Ramírez, P.E. Tapia-González, N. Ferguson, M. Brennan, B. Tang, B. Recent advances in shock vibration isolation: An overview and future possibilities. *Applied Mechanics Reviews*, **71**(6), 1-23, 2019.

[2] D. Losanno, H.A. Hadad, G. Serino, Seismic behavior of isolated bridges with additional damping under far-field and near fault ground motion. *Earthquakes and Structures*, **13**(2), 119-130, 2017.

[3] D. Losanno, M. Spizzuoco, G. Serino, Optimal design of seismic isolation systems for simply supported bridges. *Earthquakes and Structures*, **7**(6), 969-999, 2014.

[4] D. Losanno, H.A. Hadad, G. Serino, Design charts for Eurocode based design procedure of elastomeric seismic isolation systems. *Soil Dynamics and Earthquake Engineering*, **119**, 488-498, 2018.

[5] D. Losanno, M. Spizzuoco, G. Serino, Design and retrofit of multi-story frames with elastic-deformable viscous damping braces. *Journal of Earthquake Engineering*, **23**(9), 1441-1464, 2019.

[6] I. Nuzzo, D. Losanno, F. Ciliento, N. Caterino, Analytical and numerical modelling of shear-link device for seismic energy dissipation in frame structures. *Engineering Structures*, **214**, 110630, 2020.

[7] P. Balaji, L. Moussa, M. Rahman, L. T. Vuia, Experimental investigation on the hysteresis behavior of the wire rope isolators. *Journal of Mechanical Science and Technology* **29**(4), 1527-1536, 2015.

[8] N. Vaiana, S. Sessa, F. Marmo, L. Rosati, A class of uniaxial phenomenological models for simulating hysteretic phenomena in rate-independent mechanical systems and materials. *Nonlinear Dynamics*, **93**(3), 1647-1669, 2018.

[9] N. Vaiana, S. Sessa, L. Rosati, A generalized class of uniaxial rate-independent models for simulating asymmetric mechanical hysteresis phenomena. *Mechanical Systems and Signal Processing*, **146**, 106984, 2021.

[10] N. Vaiana, D. Losanno, N. Ravichandran, A novel family of multiple springs models suitable for biaxial rate-independent hysteretic behavior. *Computers and Structures*, **244**, 106403, 2021.

[11] Ayre, R.S. Engineering Vibrations, Mc. Graw Hill New York, 2002.